

The “DLR Crash Report”: Towards a Standard Crash-Testing Protocol for Robot Safety - Part I: Results

Sami Haddadin, Alin Albu-Schäffer, Mirko Frommberger, Jürgen Rossmann, and Gerd Hirzinger

Abstract—After analyzing fundamental impact characteristics of robot-human collisions in our previous work, the intention in the present paper is to augment existing knowledge in this field, verify previously given statements with standardized equipment of the German Automobile Club (ADAC), and provide a crash-test report for robots in general. Various new insights are achieved and a systematic and extensive set of data is provided. The presented work is divided into two papers. The main purpose of *Part I* is to give, similarly to reports known from the automobile world¹, a fact based and result oriented view on our newest robot crash-test experiments. In *Part II* detailed discussions of the results listed in the present paper and recommendations towards a standard crash-test protocol for robot safety are carried out.

I. INTRODUCTION

As Asimov already noted very early, safety has priority if robots are close to humans [1]. Ensuring this safety leads to various aspects ranging from preventing electrical threats to coping with human mistakes. In this paper we provide standardized crash-test results for various aspects of physical human-robot contact and their related injury potential. In Fig. 1 we give a first organization of relevant contact scenarios which potentially lead to human injury. At this point we differentiate between *unconstrained impacts*, *clamping in the robot structure*, *constrained impacts*, *partially constrained impacts*, and resulting *secondary impacts*. Please note that in Fig. 1 no differentiation between blunt or sharp contact shall be made since the contact scenario itself stays untouched in this context. In this paper we focus on blunt impacts as a continuation of our previous work in [2], [3], [4]. To keep the discussion focused we treat only the direct consequences caused by the physical contact between robot and human. An in-depth analysis of *secondary impacts* will mainly be left for future research. Since *clamping in the robot structure* is basically equivalent to *constrained impacts* and *partially constrained impacts* a separate analysis will not be carried out at this point.

In our previous work we performed free blunt impact experiments with the DLR Lightweight Robot III (LWRIII) [2] and these proved to be non-critical from a safety point of view. As the only possibly dangerous blunt contact situation for the LWRIII we identified by simulation the clamping close to a singularity [5]. Therefore, we evaluate this situation with standardized equipment in this paper. Moreover, we aim at providing a general procedure for evaluating

S. Haddadin, A. Albu-Schäffer, Mirko Frommberger, and G. Hirzinger are with Institute of Robotics and Mechatronics, DLR - German Aerospace Center, Wessling, Germany sami.haddadin@dlr.de, alin.albu-schaeffer@dlr.de, gerd.hirzinger@dlr.de
Jürgen Rossmann is with Institute of Man-Machine-Interaction, Rheinisch-Westfälische Technische Hochschule Aachen (RWTH), Aachen, Germany rossmann@mmi.rwth-aachen.de

¹A well known example from Germany is the ADAC Motorwelt.

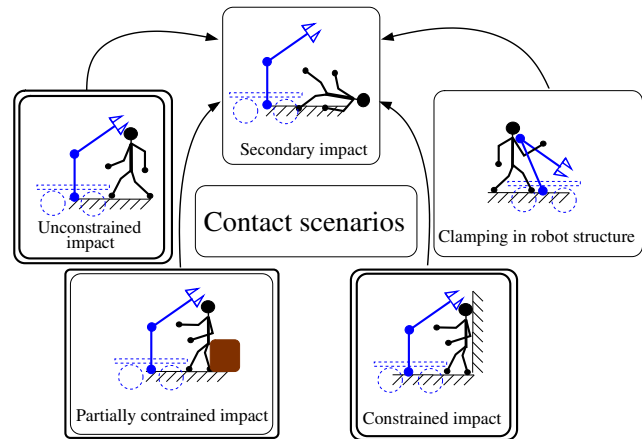


Fig. 1. Classification of undesired contact scenarios between human and robot. Generally, one can differentiate between *free impacts*, *clamping in the robot structure*, *constrained impacts*, *partially constrained impacts*, and resulting *secondary impacts*. In this distinction we do not differentiate between blunt or sharp contact since the contact *situation* stays untouched in this context. The *unconstrained impact* is characterized by being a situation in which only the robot and human are directly involved into the collision. *Clamping in the robot structure* is e.g. a situation in which a human arm is being crushed between two link segments of an articulated manipulator. The case of a *partially constrained impact* is characterized by only a part of the human being clamped which is not directly in contact with the robot (in contrast to *constrained impacts*). This causes e.g. shearing and potentially large torques on the human body at the shearing point. Apart from the direct effects of collisions, *secondary impacts* may cause further injuries, potentially leading to even larger injuries than by the direct impact itself (please note that in the pictogram only one example of this type is given). Of course a combination or sequential order of the contact types is possible as well. An example could be a human that is standing in some distance in front of a barrier (e.g. a table) being hit by the robot in free space and then being partially clamped against the object.

blunt impact injury for robotic systems. Hence, a next set of experiments was carried out with considerably heavier industrial robots². These experiments provide a feeling for the relevant situations and their parameterization in terms of velocity and robot mass, leading to suggestions for a test procedure. By anticipating the detailed discussion from *Part II* one can say that, for evaluating a particular robot, one would start with free impacts and increasingly constrain the dummy until safety thresholds are clearly exceeded for the given robot and for the relevant body parts. Full constrained impacts and singularity clamping can then be done for those robots passing the first tests, for achieving a complete blunt contact evaluation. We decided to conduct in this paper various experiments of blunt impacts with the

²We performed in previous work some of these tests with non-standardized setups for preliminary concept validation [3], [4].

industrial robots KUKA KR6, KUKA KR500, and with the LWRIII. We provide a large amount of experimental results gained from blunt impacts with a frontal Hybrid III crash-test dummy (HIII)³. Following test scenarios are evaluated in this paper:

- Head impacts
 - Dynamic unconstrained head impacts and their influence on the head, neck, and chest with the 235 kg-robot KR6 and the 2350 kg-robot KR500⁴.
 - Quasistatic constrained head impacts with the 15 kg-robot LWRIII.
 - Partial clamping during head impacts and their influence on the head, neck, and chest with the KR500.
- Chest impacts
 - Dynamic unconstrained chest impacts and their influence on the head, neck, and chest with the KR6 and the KR500.
 - Quasistatic constrained chest impacts with the LWRIII

We evaluated all injury criteria for the head, neck, and chest that are measurable with the used dummy type. Furthermore, impact forces are obtained for the evaluation of facial fractures of the mandible and the frontal bone. Generally, the purpose of this work is to

- 1) Understand the general injury mechanisms and severity behind blunt human-robot impacts.
- 2) Propose procedures for a standardized crash-testing protocol, i.e. clarify how the concept of crash-testing is applicable to any kind of robot.
- 3) Provide safety tolerance values depending on robot velocity to maximize under the safety constraint the performance of applications (e.g. incorporating manual guidance of industrial robots). Cycle times can be optimized with the knowledge gained from such experiments.

The last aspect is especially relevant for industrial robot manufacturers due to the fact that future applications are focusing on physical interaction between humans and industrial robots with additional sensors as e.g. a force-torque sensor in the wrist. It is clear and was already analyzed in [4] that constrained impacts with heavy-duty industrial robots are very dangerous indeed while unconstrained impacts are by far less critical. Therefore, the (time-)optimal performance can be achieved if clamping can be excluded in the particular application. This in turn requires a precise and careful design of the workstation to remove possibilities of the human getting pinched as much as possible.

Similar to the standard crash-test procedures in the automobile industry we want to give experimental data and suggestions for standard impacts with crash-test dummies as one part of future standardized robot safety evaluation. As

³Please note that we do not evaluate any low-severity soft-tissue injury, since this is not measurable with standard crash-test dummies. Although it is possible to evaluate **blunt** abdominal injury with certain dummies it is not feasible to investigate skin injury as lacerations, contusions, or abrasions with them. However, for the interested reader regarding this we refer to our previous work in [6], describing results on stabbing and cutting.

⁴The number in the names of the KUKA robots indicate the maximum nominal payload.

is explained in *Part II* we propose various standard blunt impact tests with

- 1) different impact directions,
- 2) sitting or standing dummy, and
- 3) defined secondary impact conditions.

II. RELATED WORK

In [7] the human pain tolerance was evaluated on the basis of human experiments. In this work the Somatic Pain was considered as a suitable criterion for determining a safety limit against mechanical stimuli.

Pioneering work on human-robot impacts under certain worst-case conditions and resulting injuries was carried out in [8] and [9], evaluating free rigid impacts at a robot speed of 1 – 2 m/s. Both contributions introduced new compliant joint design concepts and made the first attempt to use the so called Head Injury Criterion (HIC) [10] to quantify the injury potential during occurring collisions⁵.

In [14] various severity indices for the head (Gadd Severity Index (GSI), Maximum Power Index (MPI), Effective Displacement Index (EDI), Revised Brain Model (RBM), Vienna Institute Index (JTI), and Maximum Mean Strain Criterion (MSC) and for the chest (Acceleration Criterion (AC), Compression Criterion (CC), and Viscous Criterion (VC) were reviewed and analyzed in simulation for the case of unconstrained impacts with a lightweight robot. The main conclusion was that during blunt impacts with such a robot basically no significant injury can be observed by means of these criteria at an impact velocity of 1 m/s. Furthermore, it was shown that a reduction in joint stiffness for an already moderately flexible robot as the LWRIII (and similar reflected inertia) is only marginally reducing the impact dynamics during a rigid impact as the one between a robot and the human head.

From the standardization body's side the ISO-10218 was introduced, defining new collaborative operation requirements for industrial robots [15]. It states that one of the following conditions always has to be fulfilled for allowing human-robot interaction: The TCP/flange velocity needs to be ≤ 0.25 m/s, the maximum dynamic power ≤ 80 W, or the maximum static force ≤ 150 N.

Further aspects concerning safety in human-robot interaction were introduced in [16]. In this work several danger indices were proposed based on the design properties of the robot. In [17] a control scheme was developed to limit the impact force of a robot by restricting the torque commands. [18] recommended various design novelties for a mobile robot with physical compliance introduced in its trunk and a passively movable base. [19] developed an integrated human-robot interaction strategy incorporating a definition of danger by means of reflected inertia, relative velocity and the distance between human and robot.

Attempts to investigate real-world threats via impact tests at standardized crash-test facilities and use the outcome to analyze safety issues during physical human-robot interaction were to our knowledge for the first time carried out in [2] up to now. In order to quantify the potential danger

⁵A correction of the initial misinterpretation in units, and thus significant overestimation of the resulting HIC, done in [8] and [9] was first carried out in [11], [2], [5] and then in [12], [13].

emanating from the DLR Lightweight-robot III (LWRIII), impact tests at the Crash-Test Center of the German Automobile Club (ADAC) were conducted and evaluated. The effect robot speed, robot mass, and constraints in the environment have on safety in human-robot impacts is analyzed in [3] and [4]. Furthermore, facial and cranial fractures were analyzed by evaluating impact forces as injury indicators since they correlate to fractures. The current paper is the consequent follow-up of this work.

After this short outline of existing approaches to analyze and achieve safety in physical human robot interaction the applied testing protocol shall now be shortly explained in order to enable the reader to properly interpret the given results. For a detailed description please refer to [2], [20].

III. INJURY EVALUATION AND TEST SETUP

In this section all evaluated biomechanical severity indices, the injury severity scale of the EuroNCAP, and the overall setup of the impact tests are described.

A. The EuroNCAP

The ADAC crash-tests are carried out according to the EuroNCAP⁶ which injury classification is based on the Abbreviated Injury Scale (AIS) [21]. The EuroNCAP, inspired by the American NCAP, is a manufacturer independent crash-test program uniting the European ministries of transport, automobile clubs and underwriting associations with respect to their testing procedures and evaluations [20]. The outcome of the tests, specified in the program, is a scoring of the measured results via a sliding scale system. Upper and lower limits for the injury potentials are often defined such that they correlate to a certain probability of AIS ≥ 3 (serious injury). Between these two values the corresponding score (injury potential) is calculated by linear interpolation. A standardized color code, which indicates injury potential is given in Tab. I.






Colorcode	Color	Injury potential
Red		Very high
Brown		High
Orange		Medium
Yellow		Low
Green		Very low

TABLE I

EURONCAP INJURY SEVERITY AND CORRESPONDING COLOR CODE.

All successive results are classified according to their EuroNCAP rating (i.e. indicated by the corresponding color from Tab. I) if such a correlation is defined. Otherwise, we give only numerical values and shortly discuss their implications by other means as outlined next.

B. Severity Indices

In Tab. II the complete list of injury indicators which are evaluated in this work and the body part they are related to are given. Many of them were introduced in [2], [3] and

⁶European National Car Assessment Protocol

Severity Index	Body part	Symbol	EuroNCAP
Contact force	head	$F_{ext}^{frontal}$	No
Contact force	head	$F_{ext}^{mandible}$	No
Head Injury Criterion	head	HIC ₃₆	Yes
Maximum res. acceleration	head	a_{max}^{head}	Yes
3 ms criterion	head	a_{3ms}^{head}	Yes
Shearing neck force	neck	F_x	Yes
Shearing neck force	neck	F_y	Yes
Tension/compression force	neck	F_z	Yes
Flexion neck torque	neck	$M_{y,OC}^{Flex}$	No
Extension neck torque	neck	$M_{y,OC}^{Ext}$	Yes
Contact force	chest	F_{ext}^{chest}	No
Compression Criterion	chest	CC	Yes
Viscous Criterion	chest	VC	Yes
3 ms Criterion	chest	a_{3ms}^{chest}	No

TABLE II

EVALUATED INJURY INDICES.

therefore we omit their definition for brevity. We evaluate various severity indices for the head, neck, and chest.

For the head the external contact force, the Head Injury Criterion (HIC), the maximum resulting head acceleration⁷, and the 3 ms criterion are determined. The analyzed neck injury indicators are the shearing neck forces, the tension/compression force, and the flexion/extension neck torques at the occipital condyles (OC). Because the calculation of the neck force criteria depend on the duration the forces are applied to the neck and the maximum force value, we chose a worst case estimate in order to ensure an upper bound. Finally, for the chest the external force, the Compression Criterion, the Viscous Criterion, and the 3 ms Criterion are evaluated. Please note that the contact force was explicitly not filtered.

Not all measured criteria are related to injury severity within the EuroNCAP as indicated in the last column of Tab. II. We evaluate them because the standardized EuroNCAP tests do not evaluate all injury mechanisms worth to be investigated in the context of safety in physical Human-Robot Interaction (pHRI). Contact forces are e.g. directly related to fractures of facial and cranial bones and are therefore an important injury type in robotics but not part of the EuroNCAP. The tolerance values for the severity indices used in the EuroNCAP can be obtained from [20]. The indices that are not included in the EuroNCAP are classified according to tolerance values provided by suitable literature. In Tab. IV-IX we use * to denote the saturation of the force sensor and – to denote a sensor failure. For indices not included in the EuroNCAP \checkmark denotes values that are not critical, $\sim\sim\sim$ values that are in between a tolerance band, and \times values that are critical by means of the tolerance limits introduced next.

⁷Please note that this quantity is evaluated according to faceform tests specified in [22]. The higher performance limit is 80 g and the lower performance limit 120 g. We evaluate this severity index for completeness since it is explicitly used if no steering airbag is fitted.

In [3] it is described that the frontal area of the HIII is appropriate for evaluating contact forces that are related to fractures of the human frontal bone⁸. The corresponding tolerance force of the frontal bone is 4 kN. Furthermore, we conducted impact tests to the chin of the dummy in order to analyze the influence of impact direction. The tolerance force of the mandible is 1.78 kN in anterior-posterior direction and 0.89 kN in lateral direction. In this paper we assume the former for the hook to the chin as a first estimate. In [23] the tolerance torque for flexion of the neck is denoted as 190 Nm.

According to [24] the maximum tolerable contact force for the chest lies within the tolerance band of [1.15 . . . 1.7] kN. For the resulting chest acceleration a maximum value of 60 g for impact intervals of more than 3 ms cumulative duration is e.g. proposed in [25]. However, it shall be noticed that the original work presented in [26], [27] noted that such an acceleration is only tolerable with a sufficient occupant restraint system⁹. Furthermore, [26] reports a volunteer that tolerated 49.2 g without any complaints.

C. Test Setup

	Quantity	Sampling time [ms]
LWRIII	external force $F_{\text{ext}} \in \mathbb{R}^1$	0.05
	joint position $\mathbf{q} \in \mathbb{R}^7$	1
	joint torque $\boldsymbol{\tau} \in \mathbb{R}^7$	1
KR6	external force $F_{\text{ext}} \in \mathbb{R}^1$	0.05
	joint position $\mathbf{q} \in \mathbb{R}^6$	12
KR500	external force $F_{\text{ext}} \in \mathbb{R}^1$	0.05
	joint position $\mathbf{q} \in \mathbb{R}^6$	12
HIII	head acceleration $\mathbf{a}_{\text{head}} \in \mathbb{R}^3$	0.05
	neck wrench $\mathcal{F} \in \mathbb{R}^6$	0.05
	chest acceleration $\mathbf{a}_{\text{chest}} \in \mathbb{R}^3$	0.05
	chest deflection $d_{\text{chest}} \in \mathbb{R}^1$	0.05

TABLE III
MEASURED QUANTITIES.

In Fig. 2 the setup for the experiments is shown and Tab. III summarizes the instrumentation of the different setups. In addition to the standard ADAC sensors, the available sensors of the robots are recorded. The reflected inertias during the impacts of the industrial robots can be obtained from [3].

IV. DYNAMIC UNCONSTRAINED HEAD IMPACTS

In Fig. 3 high-speed recordings of a head impact at full speed are shown to visualize the dynamics of such an impact¹⁰. The robot is commanded such that it hits the dummy

⁸On the other hand, other contact areas of the dummy head are not suitable because they tend to be much stiffer than the corresponding human facial/cranial bone.

⁹The occupant restraint system is the entire equipment that belongs to the passive safety in an vehicle. Its purpose is to fix the vehicle occupant on his seat.

¹⁰Many tests described in this paper can be viewed in the attached video.

in the face in outstretched configuration while rotating about the first axis. The head is accelerated, followed by the neck being bended while the torso starts moving delayed due to the higher inertia and the elastic coupling to the head. The entire contact phase is over after ≈ 100 ms. The following motion of the dummy without having contact with the robot ends in a secondary impact on the floor. In this particular case the robot stops moving due to an exceedance of the nominal gear torque of the robot, triggered based on motor current monitoring. The collision tests were carried out at various Cartesian impact speeds ranging from 0.2 m/s to 4.2 m/s. Contact forces range up to 5 kN. Unfortunately, at very high velocities the force sensor saturated (indicated by * in the tables).

In Tab. IV the results for the unconstrained frontal impacts with the KR6 and KR500 are given. The correlation to injury severity by means of the EuroNCAP is indicated by the underlying color. In general, it can be noted that very high robot velocities have to be achieved in order to exceed the threshold from *very low* to *low* injury for all severity indices. Only at maximum velocity the HIC is slightly above the threshold value of 650 but at the same time still significantly below 1000 which denotes the critical value for this indicator. For neck shearing along the x -direction very high values are achieved which correlate (in our worst-case assumption) to *very high* injury and for the forces in tension/compression only for the KR6 the threshold from *very low* to *low* injury severity is crossed. For all other EuroNCAP injury indicators the observed potential injury stays within the *green* area. For comparison, the same measurements for the LWRIII can be found in [2].

In Tab. V the results for the unconstrained hook to the chin with the KR6 are given. The dummy is hit in cranial direction¹¹ up to a maximum velocity of 3.6 m/s. All criteria are in the *very low* area except for the maximum resulting head acceleration $a_{\text{max}}^{\text{head}}$ at 3.6 m/s which is however still in the *low* injury severity range. Furthermore, the flexion torques are far below 190 Nm and thus subcritical. Concerning fracture of the mandible it can be stated that the contact force at 1.8 m/s is already slightly above the threshold force and for higher velocities a clear exceedance is observed. However, please take into consideration that the human chin behaves quite differently and is not rigidly attached to the cranium as for the HIII. Furthermore, the interface stiffness is presumably far too high as indicated by investigations in [28]. In future work we will investigate biomechanical faces as e.g. applied in studies as [29] and developed in [30].

V. QUASISTATIC CONSTRAINED HEAD IMPACTS

In [5] the problem of quasistatic constraint impacts near singularities was pointed out. Theoretically, a robot is able to exert infinitely large forces at the tip in the singular z -direction (see Fig. 2), while driving through the singularity. The worst-case seems to be the classical reconfiguration from “elbow up” to “elbow down”. In Fig. 2 such a situation is depicted. We mounted the LWRIII horizontally and adjusted the position of the dummy such that it touched the robot at a certain distance from the singularity, labeled d_s . The robot moves from its initial position at maximum joint velocity in

¹¹See also the attached video.

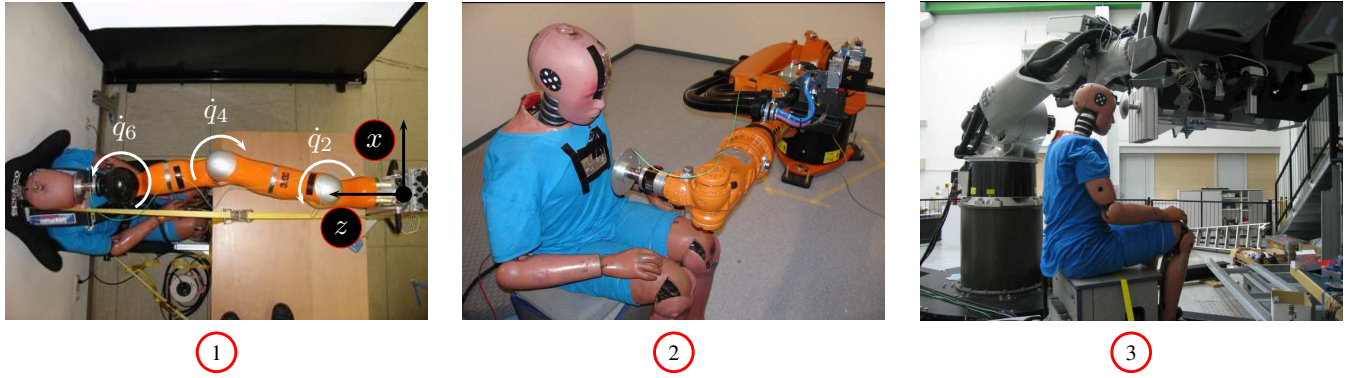


Fig. 2. Setup for the impact tests with the LWRIII (①, view from above), the KR6 (②, side view), and the KR500 (③, side view). Since for the LWRIII dynamic impacts were already analyzed in [2] we analyzed constrained impacts close to a singularity, where it is theoretically possible even for a low inertia robot to become severely dangerous. The industrial robots were tested for an outstretched configuration in order to achieve very high Cartesian velocities. The contact force is measured with a high bandwidth crash sensor. The contact geometry is defined by an aluminum impactor with radius $r_I = 120$ mm.

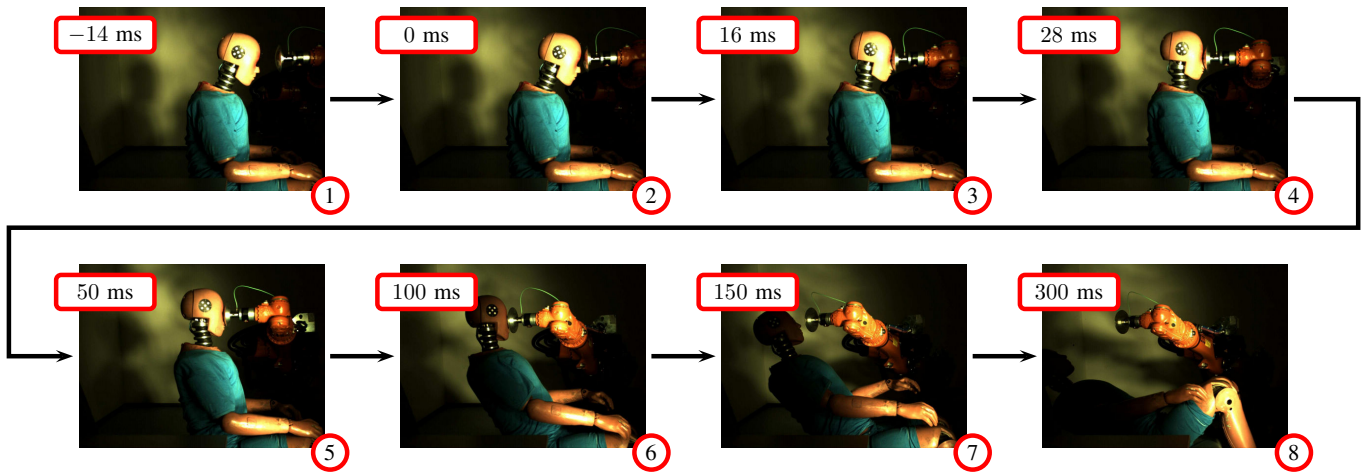


Fig. 3. High-speed recordings of an unconstrained head impact test with the KR6 and a Hybrid III dummy at 4.2 m/s.

Exp. Nr.	Robot	Strategy	d_s [mm]	F_{\max}^{static} [N]	F_{\max}^{peak} [N]
L13	LWRIII	0	10	0	✓692
L14		0	10	674	✓1244
L15		1	10	277	✓540
L16		2	10	0	✓590
L19		0	5	0	✓1593
L17		1	5	256	✓505
L18		2	5	0	✓617

TABLE VI
CONSTRAINED QUASISTATIC HEAD IMPACTS WITH THE LWRIII.

joint 4 and half the velocity in joint 2 and 6, c.f. Fig. 2. The resulting trajectory is a straight line with constant orientation in z -direction. Therefore, the robot is programmed to pass the singularity in its outstretched configuration.

In addition to commanding the described trajectory and evaluating the resulting injury we tested our collision detection and reaction for the LWRIII during this worst-case for

detection sensitivity. Our algorithm introduced and evaluated in [31], [32] uses the joint torque measurements of each joint, a good dynamics model of the robot, and the motor position sensing to generate a disturbance signal which is an estimation of the real external torques. Since in z -direction the sensitivity of this algorithm practically goes to zero close to the singularity [5], it is necessary to quantify the still achievable benefit for such a situation. The collision detection was evaluated with two reaction strategies:

- 1) Stop the robot immediately by setting the desired position to the actual position at the moment of detection.
- 2) Switch to torque control with gravitation compensation.

Strategy 0 denotes “Do not react!”. Due to the constrained environment it is not possible to measure any criterion for the head with the HIII. Therefore, only the contact force is left for evaluation. High quasistatic forces¹² can be achieved for this impact type as shown in Tab. VI. For the experiments L13 and L19 the robot is able to pass the singularity

¹²Because the robot approaches a singularity the Cartesian velocity which defines the impact velocity is quite low and therefore the contact has no typical impact characteristics anymore.

Exp. Nr.	Robot	\dot{x}_R [m/s]	$F_{\text{ext}}^{\text{frontal}}$ [N]	HIC	$a_{\text{max}}^{\text{head}}$ [g]	$a_{3\text{ms}}^{\text{head}}$ [g]	F_x [N]	F_z [N]	$M_{y,OC}^{\text{Flex}}$ [Nm]	$M_{y,OC}^{\text{Ext}}$ [Nm]
11	KR6	0.2	✓118	0.03	1.61	1.53	94.09	-165.73	✓1.93	-2.41
12		0.7	✓783	2.22	13.40	11.00	181.59	-430.26	✓7.77	-7.15
13		1.0	✓1306	6.72	23.52	16.55	320.18	-739.41	✓13.74	-8.61
6		1.3	✓1875	16.65	37.78	20.79	469.45	-861.60	✓25.34	-10.34
7		1.3	✓1766	16.88	37.53	20.82	409.32	-591.72	✓27.42	-1.18
14		1.5	✓2208	25.53	45.64	23.84	476.36	-908.09	✓29.02	-11.50
15		2.0	✓3426	64.36	77.16	25.23	710.72	-1554.63	✓42.96	-13.84
8		2.1	✓3976	96.42	93.25	25.07	691.03	-1483.54	✓45.37	-11.60
9		3.2	×5006*	344.07	167.71	21.71	949.87	-1359.89	✓67.96	-3.45
10		4.2	×5069*	671.98	213.98	38.45	1428.58	-2856.93	✓98.12	-4.09
<hr/>										
26	KR500	0.2	✓136	0.04	1.91	1.85	120.69	-86	✓0.54	-2.33
32		0.3	✓168	0.07	2.56	2.45	132.53	-88	✓0.67	-2.80
27		0.5	✓420	0.72	7.21	6.58	112.9	165	✓1.94	-5.03
28		0.7	✓798	3.10	14.87	12.53	215.93	-335	✓6.64	-6.75
29		1.0	✓1200	7.95	23.46	18.10	248.63	-375	✓11.19	-7.31
23		1.2	✓1967	17.82	35.37	24.43	407.28	-899	✓19.47	-11.51
30		1.5	✓2219	28.10	44.96	27.35	493.12	-958	✓22.22	-12.58
24		2.0	×4020	93.77	80.04	38.23	627.23	-1121	✓43.78	-7.99
31		2.0	✓3043	63.33	67.27	33.17	522.13	-758	✓30.48	-29.95
25		3.1	×4965*	248.18	141.48	47.97	967.44	-1575	✓66.22	-22.65
22		4.1	×4963*	560.00	203.66	40.56	1350.79	-2012	✓105.06	-12.35

TABLE IV
HEAD IMPACT EXPERIMENTS WITH THE KR6 AND THE KR500.

Exp. Nr.	Robot	\dot{x}_R [m/s]	$F_{\text{ext}}^{\text{mandible}}$ [N]	HIC	$a_{\text{max}}^{\text{head}}$ [g]	$a_{3\text{ms}}^{\text{head}}$ [g]	F_x [N]	F_z [N]	$M_{y,OC}^{\text{Flex}}$ [Nm]	$M_{y,OC}^{\text{Ext}}$ [Nm]
2	KR6	0.9	✓755	1.48	11.76	9.14	270	417	✓18.26	-9.82
1		1.0	✓965	2.80	16.61	11.53	350	471	✓22.52	-10.63
3		1.8	×1871	12.11	34.21	17.70	525	962	✓30.07	-17.53
4		2.7	×3128	38.92	62.59	25.78	764	1427	✓44.26	-24.60
5		3.6	×4938*	96.64	91.61	44.27	991	2564	✓48.36	-28.36

TABLE V
UNCONSTRAINED HOOK TO THE CHIN WITH THE KR6.

without exceeding its maximum nominal joint torques¹³. For $d_S = 5$ mm the robot still moves through the singularity and achieves a maximum quasistatic contact force of 1593 N. However, this is still far below the tolerance force of the frontal bone. The collision detection and reaction can reduce the occurring contact forces by 44 % for $d_s = 10$ mm and by 68 % for $d_s = 5$ mm.

VI. DYNAMIC UNCONSTRAINED CHEST IMPACTS

In Table VII the results for the unconstrained frontal chest impacts with the KR6 and KR500 are listed. Apart from the CC and the external chest force all criteria are subcritical over the entire range of impact velocities. The chest

¹³Please note that L13 was not using a tension belt which reduces the effective value of d_S because the seat can give in. For the other experiments a belt was used.

compression reaches for 4.2 m/s with the KR6 and 4.1 m/s with the KR500 potentially lethal values. Forces measured during experiments 19, 20, 36 are within the tolerance band and for 21, 37, 38 the tolerance values are clearly exceeded. The tolerable impact force for the chest¹⁴ is exceeded for 4.2 m/s for the KR6 and already at 2 m/s for the KR500.

VII. QUASISTATIC CONSTRAINED CHEST IMPACTS

In Table VIII the results of the quasistatic constrained impact of the LWRIII with the HIII chest are shown. The distance to singularity d_S varies from 20 mm to 80 mm, producing a maximum chest deflection (CC) of -11.95 mm at $d_s = 75$ mm. At $d_s = 80$ mm the maximum joint torques of the robot are exceeded which triggers a low-level safety feature to engage the brakes of the robot. This

¹⁴Please note this is a force humans can tolerate without suffering injury.

Exp. Nr.	Robot	\dot{x}_R [m/s]	$F_{\text{ext}}^{\text{chest}}$ [N]	CC [mm]	VC [m/s]	$a_{3\text{ms}}^{\text{chest}}$ [g]	HIC	$a_{3\text{ms}}^{\text{head}}$ [g]	F_x [N]	$M_{y,OC}^{\text{Flex}}$ [Nm]	$M_{y,OC}^{\text{Ext}}$ [Nm]
16	KR6	0.2	✓215	2.68	0.00	✓0.41	0.00	0.40	-17.20	✓1.04	-0.14
17		0.7	✓685	7.63	0.00	✓7.95	0.15	1.89	-67.10	✓4.61	-0.59
18		1.0	✓876	10.56	0.01	✓4.80	0.45	2.86	-141.08	✓7.19	-0.92
19		1.5	~~~~1156	13.97	0.02	✓2.51	1.03	4.02	-145.18	✓9.94	-2.55
20		2.0	~~~~1528	19.06	0.04	✓3.80	2.16	5.26	-190.13	✓14.49	-5.61
21		4.2	×3277	51.28	0.41	✓8.99	16.89	12.40	-400.71	✓37.89	-18.82
33	KR500	0.2	✓185	3.13	0.00	✓0.38	0.01	0.53	-23.78	✓1.45	-0.12
34		0.7	✓551	4.54	0.00	✓1.94	0.29	2.86	60.56	✓8.45	-1.60
35		1.0	✓847	7.44	0.01	✓4.15	0.77	4.37	56.03	✓12.37	-3.03
36		1.5	~~~~1400	14.29	0.02	✓5.10	2.7	7.43	-93.30	✓15.65	-3.88
37		2.0	×1939	22.82	0.05	✓5.36	4.09	6.70	-261.30	✓20.43	-6.13
38		4.1	×3962	57.89	0.41	✓36.93	53.26	24.88	-513.53	✓32.25	-23.72

TABLE VII
UNCONSTRAINED CHEST IMPACT EXPERIMENTS WITH THE KR6 AND THE KR500.

Exp. Nr.	Robot	Strategy	d_S [mm]	$F_{\text{max}}^{\text{static}}$ [N]	$F_{\text{max}}^{\text{peak}}$ [N]	CC [mm]
L8	LWRIII	0	20	0	✓379	-3.42
L9		1	20	180	✓300	-2.34
L10		2	20	0	✓332	-2.67
L1		0	40	-	-	-6.15
L2		1	40	130	✓291	-1.86
L3		2	40	0	✓300	-2.19
L4		0	60	0	✓859	-9.22
L11		0	70	0	✓995	-11.38
L12		0	75	0	✓1043	-11.95
L7		0	80	425	✓824	-7.59
L5		1	80	92	✓263	-1.79
L6		2	80	0	✓287	-1.99

TABLE VIII
QUASISTATIC CONSTRAINED CHEST IMPACTS WITH THE DLR-LWRIII.

shows that (with a granularity of 5 mm) the worst-case for this robot lies without collision detection and reaction at a distance to singularity of $d_S^{wc} = 75$ mm. The corresponding contact force of 1.04 kN is below the maximum tolerable threshold of the chest and the CC is constantly subcritical in the *very low* region. Similar to the constrained head impacts the reactive strategies reduce the contact force and the CC considerably. Even at the configuration closest to the singularity $d_S = 20$ mm (meaning lowest detection sensitivity of all measurements) the robot is able to react effectively.

VIII. PARTIALLY CONSTRAINED DYNAMIC HEAD IMPACTS

Table IX lists the evaluated injury indices for partially constrained impacts. In this experiment the dummy was sitting in front of a barrier which height varied from 80 mm to 160 mm, c.f. Fig. 4. The impact criteria, such as HIC, have similar values to the ones obtained for the unconstrained dynamic impact presented in Sec. IV. The influence of the barrier mainly results in larger neck forces and torques.

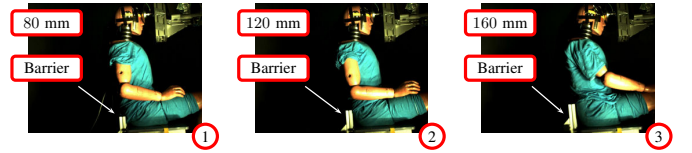


Fig. 4. Partially constrained impact. A barrier was mounted on the back of the dummy with 80 mm (①), 120 mm (②), and 160 mm height (③).

Please note that experiment 43 is presumably not comparable to the others because the impact direction had a significant lateral component.

IX. CONCLUSION & OUTLOOK

Part I of this work provided a rich basis of impact testing results for future robot crash-test protocols. We measured numerous injury indicators with standard automobile crash-testing equipment and rated them according to an established crash-testing protocol. Robots of entirely different weight and at various velocities are evaluated for typical and relevant situations. Furthermore, the usage of a HIII gave us the ability to analyze full body responses and thus evaluate what happens at remote locations of the body (e.g. the head neck complex) during an impact with another body part (e.g. the chest). The resulting data basis will help to understand the mechanisms behind injuries in robotics and contribute to a fact based discussion of safety in physical human-robot interaction. Furthermore, this paper is intended as a proposal of how future impact experiments can be presented in a comparable and descriptive way, similar to already established procedures in the automobile industry. *Part II* will discuss the obtained results in detail and give conclusions on how to use them in a possible standardized way. A **video** illustrating and supporting key aspects proposed and explained in the paper is attached.

Exp. Nr.	Robot	h_B [mm]	\dot{x}_R [m/s]	$F_{ext}^{frontal}$ [N]	HIC	α_{max}^{head} [g]	α_{3ms}^{head} [g]	F_x [N]	F_z [N]	$M_{y,OC}^{Flex}$ [Nm]
39	KR500	80	2.0	✓2945	59.48	59.76	36.35	563.42	-479.90	✓37.45
41		120	2.0	✓3059	67.98	67.98	34.83	476.76	-471.44	✓29.02
43		160	2.0	✓2795	40.87	53.67	30.80	482.06	-1137.25	✓16.74
40		80	4.1	×4950*	419.38	170.64	47.67	975.13	-670.60	✓68.07
42		120	4.1	×4978*	408.31	170.45	47.27	864.13	-913.97	✓53.04
44		160	4.1	×5165*	500.37	195.54	45.13	1268.34	-1296.91	✓93.98

TABLE IX

PARTIALLY CONSTRAINED HEAD IMPACT EXPERIMENTS WITH THE KR500. THE BARRIER HEIGHT h_B RANGES UP TO 160 MM.

ACKNOWLEDGMENT

This work has been partially funded by the European Commission's Sixth Framework Programme as part of the project PHRIENDS under grant no. 045359. We would like to thank the ADAC and especially Daniel Schindler for their excellent collaboration and for contributing such valuable expertise. Furthermore, we would like to thank KUKA Roboter GmbH for their financial support and especially Dr. Tim Guhl for his help with the experiments.

REFERENCES

- [1] I. Asimov, *The Caves Of Steel, A Robot Novel*, 1954.
- [2] S. Haddadin, A. Albu-Schäffer, and G. Hirzinger, "Safety Evaluation of Physical Human-Robot Interaction via Crash-Testing," *Robotics: Science and Systems Conference (RSS2007)*, pp. 217–224, 2007.
- [3] —, "The Role of the Robot Mass and Velocity in Physical Human-Robot Interaction - Part I: Unconstrained Blunt Impacts," in *IEEE Int. Conf. on Robotics and Automation (ICRA2008)*, Pasadena, USA, 2008, pp. 1331–1338.
- [4] —, "The Role of the Robot Mass and Velocity in Physical Human-Robot Interaction - Part II: Constrained Blunt Impacts," *IEEE Int. Conf. on Robotics and Automation (ICRA2008)*, Pasadena, USA, pp. 1339–1345, 2008.
- [5] —, "Safe Physical Human-Robot Interaction: Measurements, Analysis & New Insights," in *International Symposium on Robotics Research (ISRR2007)*, Hiroshima, Japan, 2007, pp. 439–450.
- [6] S. Haddadin, A. Albu-Schäffer, A. De Luca, and G. Hirzinger, "Evaluation of Collision Detection and Reaction for a Human-Friendly Robot on Biological Tissue," in *IARP International Workshop on Technical challenges and for dependable robots in Human environments (IARP2008)*, Pasadena, USA. [Online]. Available: www.robotic.de/Sami.Haddadin
- [7] Y. Yamada, Y. Hirasawa, S. Huand, and Y. Umetani, "Fail-Safe Human/Robot Contact in the Safety Space," *IEEE Int. Workshop on Robot and Human Communication (RO-MAN1996)*, pp. 59–64, 1996.
- [8] A. Bicchi and G. Tonietti, "Fast and Soft Arm Tactics: Dealing with the Safety-Performance Trade-Off in Robot Arms Design and Control," *IEEE Robotics & Automation Mag.*, vol. 11, pp. 22–33, 2004.
- [9] M. Zimm, O. Khatib, and B. Roth, "A New Actuation Approach for Human Friendly Robot Design," *Int. J. of Robotics Research*, vol. 23, pp. 379–398, 2004.
- [10] J. Versace, "A Review of the Severity Index," *Proc 15th Stapp Conference*, vol. SAE Paper No.710881, pp. pp. 771–796, 1971.
- [11] S. Haddadin, A. Albu-Schäffer, and G. Hirzinger, "Approaching Asimov's 1st Law," *HRI Caught on Film, Proceedings of the 2nd ACM/IEEE International Conference on Human-Robot Interaction Washington DC*, pp. 177–184, 2007.
- [12] A. Bicchi, M. Bavaro, G. Boccadamo, D. De Carli, R. Filippini, G. Grioli, M. Piccigallo, A. Rosi, R. Schiavi, S. Sen, and G. Tonietti, "Physical human-robot interaction: Dependability, safety, and performance," in *Int. Workshop on Advanced Motion Control (AMC2008)*, 2008, pp. 9–14.
- [13] D. Shin, I. Sardellitti, and O. Khatib, "Hybrid actuation approach for human-friendly robot design," in *IEEE Int. Conf. on Robotics and Automation (ICRA 2008)*, Pasadena, USA, 2008, pp. 1741–1746.
- [14] S. Haddadin, "Evaluation Criteria and Control Structures for safe Human-Robot Interaction," Master's thesis, Technical University of Munich (TUM) & German Aerospace Center (DLR), 12 2005.
- [15] ISO10218, "Robots for industrial environments - Safety requirements - Part 1: Robot," 2006.
- [16] K. Ikuta, H. Ishii, and M. Nokata, "Safety Evaluation Method of Design and Control for Human-Care Robots," *Int. J. of Robotics Research*, vol. 22, no. 5, pp. 281–298, 2003.
- [17] J. Heinzmann and A. Zelinsky, "Quantitative Safety Guarantees for Physical Human-Robot Interaction," *Int. J. of Robotics Research*, vol. 22, no. 7-8, pp. 479–504, 2003.
- [18] H.-O. Lim and K. Tanie, "Human Safety Mechanisms of Human-Friendly Robots: Passive Viscoelastic Trunk and Passively Movable Base," *Int. J. of Robotics Research*, vol. 19, no. 4, pp. 307–335, 2000.
- [19] D. Kulic and E. Croft, "Pre-Collision Strategies for Human Robot Interaction," *Autonomous Robots*, vol. 22, no. 2, pp. 149–164, 2007.
- [20] EuroNCAP, "European Protocol New Assessment Programme - Assessment Protocol and Biomechanical Limits," 2003.
- [21] AAAM, *The Abbreviated Injury Scale (1990) Revision Update 1998*. Des Plaines/IL, 1998.
- [22] EuroNCAP, "European Protocol New Assessment Programme - Frontal Impact Testing Protocol," 2004.
- [23] H. Mertz and L. Patrick, "Strength and Response of the Human Neck," *Proceedings of the 15th Stapp Car Crash Conference (STAPP1971)*, pp. 207–255, 1971.
- [24] L. Patrick, "Impact Force Deflection of the Human Thorax," *SAE Paper No.811014, Proc. 25th Stapp Car Crash Conference*, pp. 471–496, 1981.
- [25] F. M. V. S. Standards, "FMVSS 208 - Occupant Crash Protection," 2004.
- [26] H. Mertz and C. Gadd, "Thoracic Tolerance to Whole-body deceleration," *Proceedings of the 15th Stapp Car Crash Conference*, pp. 135–157, 1971.
- [27] J. Stapp, "Voluntary Human Tolerance Levels," *Proceedings of Impact Injury and Crash Protection*, pp. 308–349, 1970.
- [28] D. L. Allsop, C. Y. Warner, M. G. Wille, D. C. Schneider, and A. M. Nahum, "Facial Impact Response-A Comparison of the Hybrid III Dummy and Human Cadaver," *SAE Paper No.881719, Proc. 32th Stapp Car Crash Conference*, pp. 781–797, 1988.
- [29] D. Viano, C. Bir, T. Walilko, and D. Sherman, "Ballistic Impact to the Forehead, Zygoma, and Mandible: Comparison of Human and Frangible Dummy Face Biomechanics," *The Journal of Trauma*, vol. 56, no. 6, pp. 1305–1311, 2004.
- [30] J. Melvin, W. Little, J. Smrcka, Z. Yonghau, and M. Salloum, "A Biomechanical Face for the Hybrid III Dummy," *Proceedings of the 39th Stapp Car Crash Conference*, 1995.
- [31] A. De Luca, A. Albu-Schäffer, S. Haddadin, and G. Hirzinger, "Collision Detection and Safe Reaction with the DLR-III Lightweight Manipulator Arm," *IEEE/RSJ Int. Conf. on Intelligent Robots and Systems (IROS2006)*, pp. 1623–1630, 2006.
- [32] S. Haddadin, A. Albu-Schäffer, A. De Luca, and G. Hirzinger, "Collision Detection & Reaction: A Contribution to Safe Physical Human-Robot Interaction," in *IEEE/RSJ Int. Conf. on Intelligent Robots and Systems (IROS2008)*, Nice, France, 2008, pp. 3356–3363.